Weak and strong coupling of photons and excitons in photonic dots

T. Gutbrod, M. Bayer, A. Forchel, and J. P. Reithmaier
Technische Physik, Universität Würzburg, Am Hubland, D-97074 Würzburg, Germany

T. L. Reinecke
Naval Research Laboratory, Washington, D.C. 20375

S. Rudin
U.S. Army Research Laboratory, Adelphi, Maryland 20856

P. A. Knipp
Christopher Newport University, Newport News, Virginia 23606
(Received 9 July 1997; revised manuscript received 12 January 1998)

The weak- and strong-coupling regimes of photons and excitons in photonic dots are studied by photoluminescence spectroscopy. Because of the three-dimensional confinement, the optical mode spectrum is split into a set of discrete states in these structures. The energies of the photon states are studied as a function of the dot size and shape. Further, we investigate the formation of cavity polaritons in photonic dots. The Rabi splitting between the polariton branches is found to depend on the lateral size of the dots and on the photon mode. These dependences are related by calculations to changes of the exciton-photon coupling resulting from photon confinement. [S0163-1829(98)00916-3]

I. INTRODUCTION

Semiconductor microcavities (MC's) are powerful tools for studying fundamental problems in light-matter interaction.[1,2] These structures consist of single or multiple quantum wells (QW's) sandwiched between two high-quality Bragg reflectors (BR's), which confine the photons along the direction normal to the BR's. The electronic excitations are controlled by the parameters of the QW's, e.g., width and composition. The optical modes, on the other hand, depend on the properties of the entire MC such as cavity length and composition of the mirrors. Thus the properties of the electronic and photonic excitations can be controlled separately by the structural design. This can lead, for example, to enhanced light-matter interaction or to a reduction of the spontaneous emission.[1–8]

The regimes of both weak and strong coupling between photonic and electronic excitations occur in these systems. In the weak-coupling case one of the excitations couples to a continuum of states of the other excitation. Then the interaction is described by Fermi's golden rule and gives rise to a linewidth and dissipation. In the regime of strong coupling, the photonic and electronic (here excitonic) excitations are fully discretized. Then the eigenstates of the system are mixed exciton-photon states, the so-called cavity polaritons, which are split in energy. The energy splitting corresponds to the vacuum Rabi splitting in atomic physics.[9,10]

In previous work on semiconductor MC's the photons were confined only in the direction parallel to the growth direction and both the excitons and the photons have continuous spectra corresponding to motion in the QW plane. Recently, photonic dots (PD's) have been fabricated, in which the photonic modes are confined in all three directions: in the vertical direction by the BR's and along the lateral directions due to the large discontinuity of the refractive index at the dot sidewalls.[11,12]

In the present work we first describe in Sec. II the photonic dot samples used in the present experiments. In Sec. III the mode spectrum of PD's is studied in the weak-coupling regime of excitons and photons. In particular, we discuss the dependence of the energies of the optical modes on the dot size and shape. In addition, we study the strong-coupling regime of excitons and photons in Sec. IV. Quasi-zero-dimensional polariton-like states are formed due to the strong coupling of the ground-state heavy-hole exciton ($1s$hh) with several confined photon modes. We investigate the size and mode dependence of the Rabi splitting in PD's. The experimental results are compared with the results of detailed numerical calculations.

II. EXPERIMENT

The MC layer structure used to fabricate the PD's was grown by molecular-beam epitaxy. The λ cavity consists of a 251-nm-wide GaAs layer in the center of which a 7-nm-wide $In_{0.14}Ga_{0.86}As$ single QW is embedded. This structure is sandwiched between two BR's consisting of 19 quarter-wave stacks of GaAs/AlAs layers on top and 21 at the bottom (on top of the substrate). In order to obtain three-dimensional photon confinement, arrays of square and circular photonic dots were fabricated:[12] The shape of the dots was defined by electron-beam lithography and the pattern was transferred into the semiconductor by dry etching. Details of the fabrication process have been given earlier.[13] The cavity was etched through the top BR and the GaAs λ cavity down to the top of the bottom BR.

Figure 1 shows scanning electron micrographs of arrays of square and circular photonic dots. The diameter of the

 © 1998 The American Physical Society

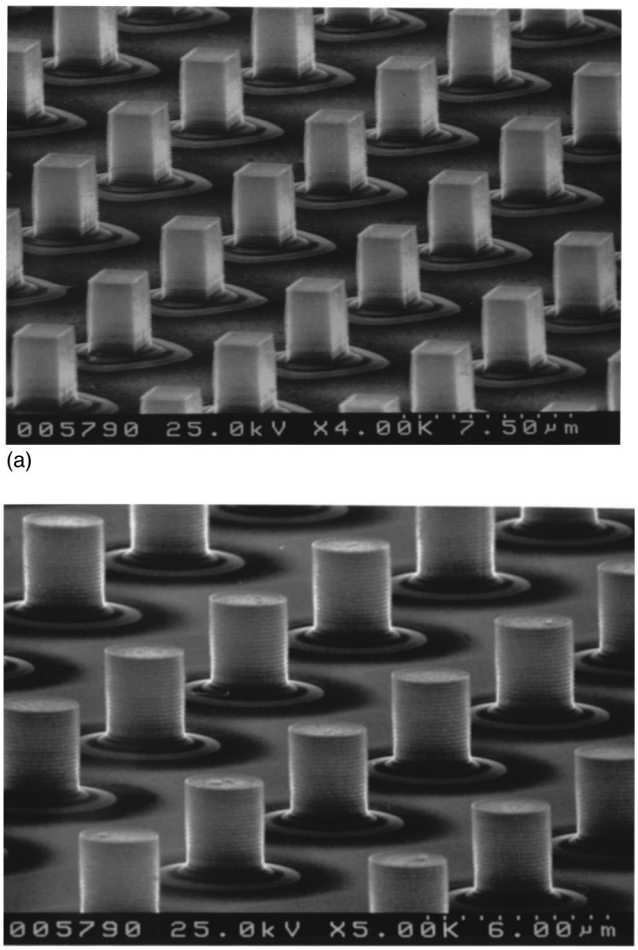

FIG. 1. Scanning electron micrographs of (a) square and (b) circular photonic dots with sizes of 2.7 μm and diameters of 2.7 μm, respectively.

circular dots is 2.7 μm and the lateral size of the square dots is 2.7 μm. On top of the structures the upper mirror consisting of alternating GaAs and AlAs layers can be seen followed by the GaAs λ cavity. The lower mirror remains basically unetched except for about one to two layers of GaAs/AlAs. The lateral spacing between adjacent dots was so large that coupling effects between the dots can be excluded.

The samples were mounted into the variable temperature insert (1.8 K$\leqslant T \leqslant$200 K) of an optical magnetocryostat ($B \leqslant 8$ T). The measurements were performed in Faraday configuration. An Ar^+ laser (514.5 nm) was used for optical excitation. The emitted light was dispersed by a monochromator ($f = 0.6$ m) and detected by a charge-coupled-device camera.

III. WEAK-COUPLING REGIME: PHOTON MODE SPECTRUM

First, we study the spectrum of optical modes in PD's, where the energy separation between the photon and the exciton is large. In this off-resonance case the excitations are only weakly coupled. Figure 2 gives photoluminescence (PL) spectra of square [Fig. 2(b)] and circular [Fig. 2(c)] PD's with varying sizes at $T = 2$ K. In order to resolve also

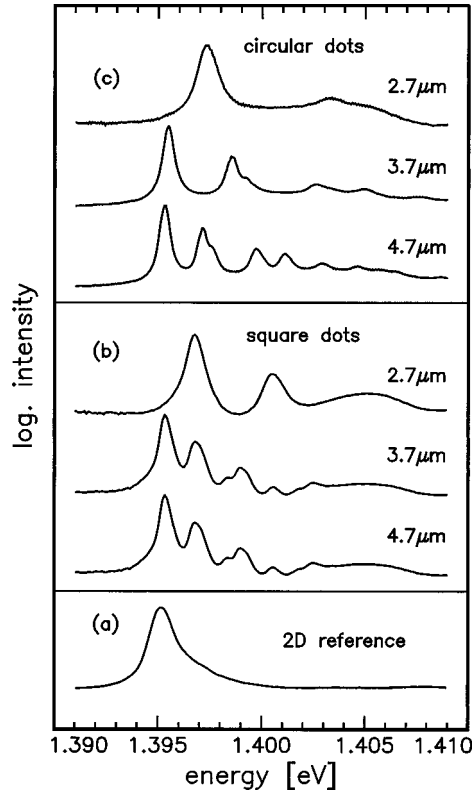

FIG. 2. PL spectra of PD's with varying lateral sizes recorded in the weak-coupling regime of excitons and photons. The spectra of (b) square dots and (c) circular dots are shown. For comparison we also show (a) the spectra of a two-dimensional reference sample.

weak spectral features the intensity is shown on a logarithmic scale. For comparison, the spectrum of a two-dimensional reference sample is also shown [Fig. 2(a)]. The main feature in this reference spectrum is the emission from the photon mode at an energy of about $E_0 = 1.395$ eV. The mode corresponds to the sharp decrease of the reflectivity in the center of the stop band of the vertical resonator. A broadening of the spectral line to higher energies is observed: The luminescence is collected within a finite solid angle, so that also emission from photon states with finite wave numbers in the cavity plane is detected and this emission causes the asymmetry of the emission line. The exciton emission is not shown in Fig. 2. It is located about 20 meV above the photon mode at $E = 1.415$ eV and due to this large exciton-photon detuning strong-coupling effects can be neglected.

In contrast to the reference sample, the emission spectra of the PD's consist of a set of sharp lines that originate from the discretization of the continuum of photon states in the cavity due to the lateral photon confinement.[14] Two features can be noted. First, the modes shift continuously to higher energies with decreasing dot size. For example, in the square dots the ground photon state in 2.7-μm-wide PD's is shifted by about 2.5 meV to higher energies. Second, the energy splitting between the different confined modes increases with decreasing size. The mode energies in the circular dots increase more strongly with decreasing size than those in the rectangular dots. For example, for the first excited photon state of 2.7-μm PD's a high-energy shift of about 5 meV is observed in square dots in comparison to 8 meV in circular dots with this diameter.

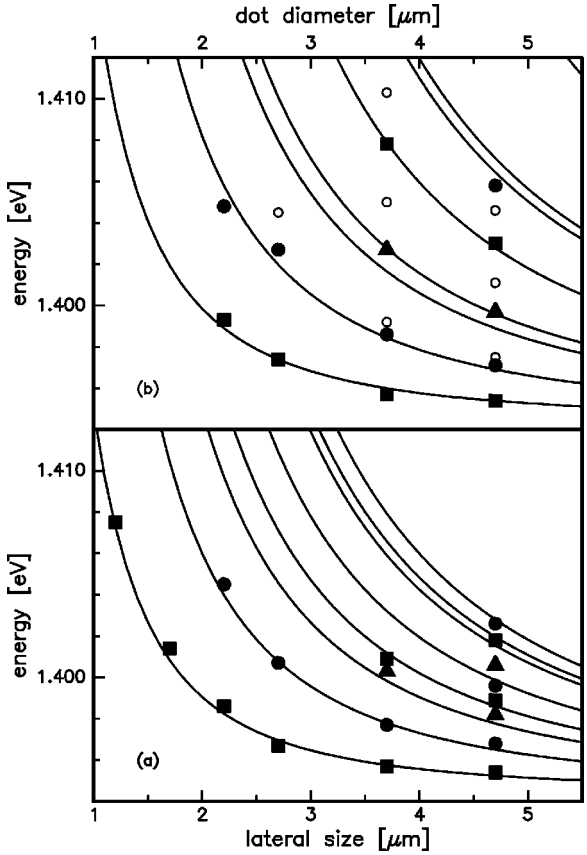

FIG. 3. Energies of the photon states in square and circular PD's as a function of the lateral size or diameter, respectively. Symbols give the experimental data, and lines the results of numerical calculations as described in the text.

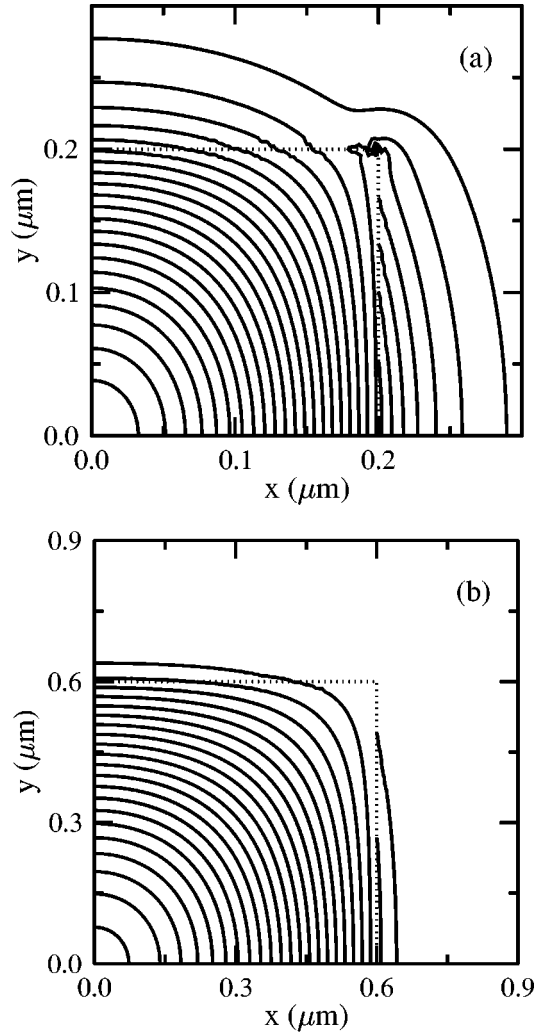

FIG. 4. Contour plots of the electric-field distributions in the cavity planes for square PD's with lateral sizes of (a) 0.4 μm and (b) 1.2 μm. Only one-quarter of the cavity plane is shown and the boundaries of the PD are indicated by the dotted lines.

The lateral size dependence of the mode energies is summarized in Fig. 3, where the energies of the photon modes are shown versus dot size for both types of cavities. The symbols give the experimental data from PL experiments for square [Fig. 3(a)] and circular [Fig. 3(b)] dots. In order to understand quantitatively the lateral confinement effects, we have made detailed calculations of the modes of these cavities. The spatial variations of the fields in the growth direction (z) correspond to an energy $\sim$1.4 eV and are considerably greater than those in the lateral directions (x,y), which correspond to the lateral confinement energies. Thus we take the fields to be separable as a product of a function of z times a function of (x,y). For the motion in the z direction a transfer matrix calculation is used. For that in the (x,y) plane numerical calculations using a ''boundary element method,'' which we have recently developed,[15–17] have been made. The modes are nearly transverse with the electric field lying mainly in the (x,y) plane and are doubly degenerate corresponding to two polarizations. The modes $(n_x,n_y,0)$ can be characterized as having (n_x,n_y) nodes in the (x,y) directions. The zero indicates the vertical field distribution in the λ cavity.[13] In order to account for the effect of the fields penetrating into the unetched mirrors below the active region, the confinement energies are taken to be the average of calculations for a system that has been etched completely through the substrate and that for an unetched system weighted by the square of the electric fields in the etched and unetched regions, with the weights taken from the transfer-matrix calculations. The results are given by the solid lines in Fig. 3.

Figure 4 gives the ground-state electric-field distributions in the photonic dot plane of square cavities for two cavity sizes: 0.4 μm [Fig. 4(a)] and 1.2 μm [Fig. 4(b)]. The field is polarized along the x direction. Only one-quarter of the cavity is shown, whose boundaries are indicated by the dotted lines. For larger sized cavities the fields are fairly well contained in the cavity. From the calculations we find that to lowest order in the parameter k_0L the states are represented by a model in which the cavity walls are taken to be perfectly reflecting and for which the energies of the modes are given by

$$E_{n_x,n_y}=\sqrt{E_0^2+\frac{\hbar^2c^2}{\varepsilon}(k_{x,n_x}^2+k_{y,n_y}^2)}, \qquad (1)$$

where $E_0=\hbar ck_0/\sqrt{\varepsilon}$ is the energy of the unetched cavity with k_0 being the corresponding wave vector. Here the lateral wave numbers are given by the simple condition $k_{i,n_i}=\pi(n_i+1)/L$, where $i=x,y$; $n_i=0,1,\ldots$, and L is the lateral cavity size. In Fig. 3(a) we show the calculated energies

for the seven lowest optical modes with lateral eigenvalues $(n_x,n_y,0)$ in order of increasing energy. These modes are (0,0,0), (1,0,0), (1,1,0), (2,0,0), (2,1,0), (3,0,0), and finally (2,2,0).

The corresponding formula for the circular cavities with perfectly reflecting sidewalls is

$$E=\sqrt{E_0^2+\frac{\hbar^2c^2}{\varepsilon}\frac{x_{n_\varphi,n_r}^2}{R^2}}, \tag{2}$$

where x_{n_φ,n_r} is the n_rth zero of the Bessel function $J_{n_\varphi}(x_{n_r,n_\varphi}r/R)$.[18] R is the radius of the circular dot. The calculated energies are shown in Fig. 3(b). Here the seven lowest states $(n_r,n_\varphi,0)$ are (1,0,0), (1,1,0), (1,2,0), (2,0,0), (2,1,0), (2,2,0), and (3,0,0).

In the case of the square dots the results of the detailed calculations given here account well for the experimental data. In the case of the circular dots we observe a splitting of the excited states, as indicated by the full symbols and the open circles. The splitting between these states increases with decreasing dot size. From electron microscopy we find that the dots are slightly elliptical with the main axis of the ellipsoids about 0.2 μm longer than the other independent axis of the dot. This breaks the circular symmetry of the dots and leads to a splitting of the excited states.

IV. STRONG-COUPLING REGIME: FORMATION OF POLARITONS

The case of strong coupling of excitons and photons when both modes come into resonance has been studied. Then the states hybridize and form cavity polaritons that repel each other in energy. Strongly coupled cavity polaritons have been observed in two-dimensional MC's.[1,2] In this case the coupling occurs between photon and exciton modes that have the same wave vector k parallel to the direction of motion in a manner similar to a bulk polariton. It has been shown that cavity polaritons exist up to room temperature due to the enhanced exciton binding energy in the QW's.[19] In addition, the Rabi splitting can be modified by applying electric or magnetic fields to the heterostructure.[20,21]

In order to obtain the resonance condition, variations of the dimensions of the vertical cavity across the sample have been used.[1] They can cause a strong variation of the photon mode energy. In addition, angle-resolved studies may be used, from which one obtains the in-plane dispersion of the polariton branches.[2] Another approach is to vary the sample temperature, which changes the exciton energy, while the energies of the photon modes have only a comparatively weak dependence on temperature. In our work, in order to obtain the exciton-photon resonance in PD's, we have varied the sample temperature. In these laterally confined structures angle-resolved studies cannot be used because, as a result of the three-dimensional confinement, the photon states have no in-plane dispersion. For a given mode the energy does not depend on the angle under which the emission is detected.

For these investigations the system parameters in the unpatterned sample have been chosen in such a way that at low temperatures ($T\leqslant 50$ K) the exciton-photon detuning is ~ 10 meV and the polariton branches are still well separated in energy. Then one branch is excitonlike and the other one is photonlike. To discretize the spectrum of electronic excitations a magnetic field B is applied normal to the QW. The exciton wave function Ψ_X is squeezed by B and thus the exciton oscillator strength f_0 is increased, which is given by $f_0\propto|\Psi_X(\vec{r}_e=\vec{r}_h)|^2$. Here $\vec{r}_e$ and $\vec{r}_h$ are the coordinates of the electron and hole.

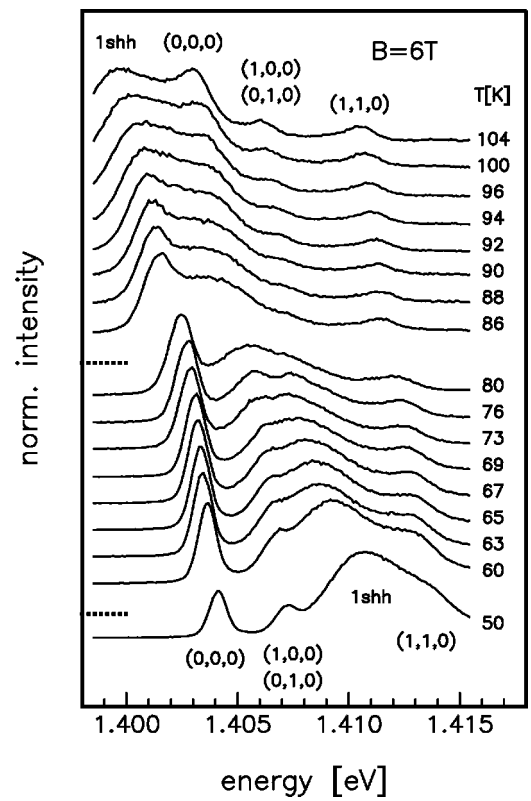

FIG. 5. PL spectra of a square PD with a size of 2.7 μm at $B=6$ T for varying temperatures (increasing from bottom to top). The spectra were recorded by using low excitation powers of 10 W cm^{-2}.

Figure 5 shows PL spectra of a PD with a lateral size of 2.7 μm for varying temperatures (increasing from bottom to top) at $B=6$ T. The low-temperature spectrum ($T=50$ K) consists of three main spectral features. The broadband at $E=1.413$ eV corresponds to the 1$s$hh exciton. The two features on the low-energy side of 1$s$hh correspond to the ground-state photon (0,0,0) and the first excited photon (1,0,0), which is degenerate with (0,1,0). The weak feature on the high-energy side of 1$s$hh is due to the second excited photon state (1,1,0).

With increasing temperature the band gap of $In_{0.14}Ga_{0.86}As$ decreases, but the energies of the photon modes are nearly independent of temperature. Thus, with increasing temperature the exciton mode can be brought subsequently into resonance with each of the lower-lying photon modes and these modes anticross as observed in Fig. 5. At temperatures of about 70 K the exciton mode comes into resonance with the first excited photon modes (0,1,0) and (1,0,0). At higher temperatures we observe the anticrossing of the exciton and the ground photon mode (0,0,0). The Rabi splitting between the polariton branches is about 2.1 meV for the (0,0,0) resonance and 1.7 meV for the degenerate (1,0,0) and (0,1,0) resonances.[22]

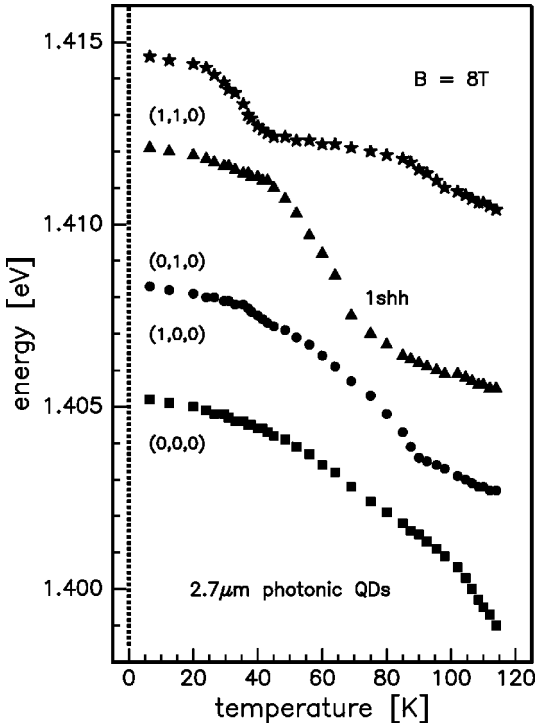

FIG. 6. Transition energies of the photon and exciton states versus temperature in PD's with lateral sizes of 2.7 μm at $B=8$ T.

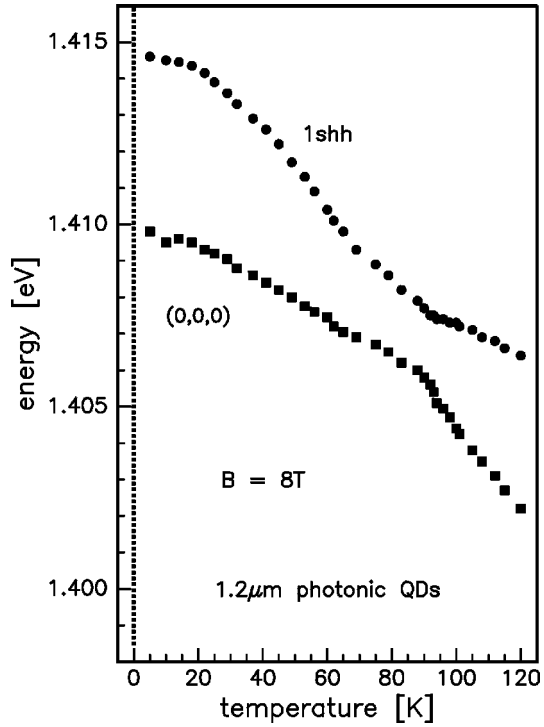

FIG. 7. Transition energies of the photon and exciton states versus temperature in PD's with lateral sizes of 1.2 μm at $B=8$ T.

Figure 6 shows the transition energies observed in 2.7-μm-wide PD's as functions of temperature at $B=8$ T. At this higher magnetic field the energy of the exciton is shifted to higher values so that also the (1,1,0) photon state lies below 1*s*hh at low temperatures. Then three anticrossings are observed with increasing temperature. The Rabi splitting increases with increasing oscillator strength[10] and therefore its values are larger at 8 T than those at 6 T. The resonance with the (0,0,0) photon state has a splitting of about 2.3 meV and that with the (1,0,0) photon state a splitting of 1.9 meV. The energy splitting of the resonance of 1*s*hh with the (1,1,0) photon mode is 1.5 meV. After anticrossing, the polariton branches exchange character, i.e., the branch of lower energy is now excitonlike and that of higher energy photonlike.[23]

Figure 7 gives the temperature variation of the transition energies in a PD with a lateral size of 1.2 μm at $B=8$ T. Due to the increased lateral confinement of the photons in comparison to the 2.7-μm-wide PD's, the photon states are shifted to higher energies. Only one photon state, the ground state (0,0,0), has an energy below 1*s*hh at low temperatures. Consequently, only one anticrossing can be observed with increasing temperature. The anticrossing occurs at about $T=90$ K and the Rabi splitting is 2.0 meV.

From Figs. 6 and 7 two noteworthy features can be seen. First, the Rabi splitting in the PD's decreases with decreasing lateral size. At $B=8$ T it is 2.3 meV for the anticrossing involving the ground photon mode in the 2.7-μm-wide cavities, whereas it is 2.0 meV in the 1.2-μm-wide cavities. Second, for cavities with a fixed lateral size the splitting between the polariton branches decreases for higher photon states as noted above for the 2.7-μm-wide PD's.

The experimentally observed Rabi splittings of several polariton branches in PD's with lateral sizes L ranging from 4.7 μm down to 1.2 μm are shown in Fig. 8(a) by symbols [squares for the (0,0,0), circles for the (0,1,0) and (1,0,0), and triangles for the (1,1,0) polaritons]. We observe for all photon modes a decrease of the Rabi splitting with decreasing lateral cavity size. The decrease is stronger the higher the eigenvalues of the photon mode. With increasing cavity size, the splittings for all modes converge to 2.5 meV for the two-dimensional reference.

An expression for the Rabi splittings in terms of the photon confinement is required in order to understand the cavity size dependence of the splitting. We have obtained the Rabi splitting both classically and quantum mechanically for a picture of N independent harmonic oscillators representing the excitons coupled to a harmonic-oscillator photon mode. The classical result is convenient for including the effects of damping of the modes. In this case the Rabi splitting is given by[24]

$$\Omega=\sqrt{\frac{\alpha^2 N}{\omega_1^2}-\frac{1}{4}(\gamma_0-\gamma_1)^2}. \tag{3}$$

Here ω_1 is the frequency of the N exciton oscillators of width γ_1, the photon oscillator width is γ_0, and α is the coupling between the exciton and photon oscillators. In the present experiments the difference of the exciton and photon widths are small compared to their coupling and will be neglected here giving $\Omega\approx\sqrt{\alpha^2 N/\omega_1^2}$. The classical photon fields then are quantized in the usual way by equating their energies to their frequencies. This gives

$$\Omega\approx\sqrt{\frac{f_0 e^2}{lm}G(L)}, \tag{4}$$

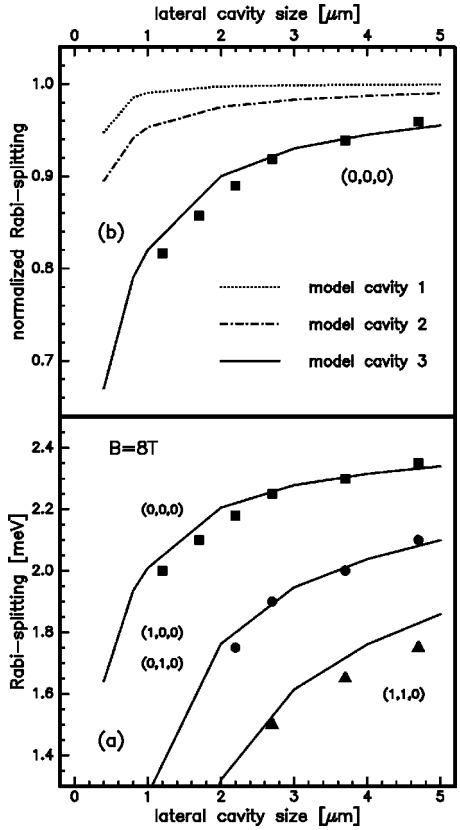

FIG. 8. (a) Rabi splittings at $B=8$ T versus lateral cavity size for different photon states. Symbols give experimental results and solid lines give results from calculations. (b) Relative decrease of Ω versus lateral cavity size for three model cavities described in the text.

where f_0 is the exciton oscillator strength per unit area and m is the corresponding mass. l is the width of the $In_{0.14}Ga_{0.86}As$ quantum well. $G(L)$ is a dimensionless function that depends on the size and the shape of the cavity and on the photon polarization. The size dependence arises from the exciton-photon interaction α, which is obtained from the absorption of light by the exciton. This size dependence will be discussed for several cavities in the following.

We begin by considering a semiconductor cavity in the shape of a parallelepiped with the property that the electric fields go to zero at the boundaries (model 1). This situation corresponds to a cavity with perfectly reflecting sidewalls. Then the electric fields are products of trigonometric functions for each spatial direction. The dependence of Ω on the lateral size L becomes simply $\Omega \propto 1/\sqrt{E(L)}$, where the energies of the confined photon states increase with decreasing size. The resulting size dependence for the polariton resonance with the (0,0,0) photon state is shown in Fig. 8(b) by the dotted line, where we have plotted the Rabi splitting normalized by Ω in the two-dimensional reference versus cavity size. In this model the size dependence is weak because in this case the fields are strongly confined and the exciton-photon interaction matrix element is affected only weakly by the confinement induced changes of the photon energies. This is also true for the higher-order optical modes.

Next we consider a semiconductor MC structure like the ones studied experimentally here except that we take the lower mirror to be etched through completely to the substrate (model 2). As discussed above, the fields are represented by functions that are separable between the z variable (the growth direction) and the x-y plane. The Rabi splitting of the ground-state polariton is given by the dash-dotted line in Fig. 8(b). The dependence of Ω on size is somewhat greater in this case than in model 1 due to the greater changes of the electric field with cavity size. The changes of field with cavity size, however, remain small (see Fig. 3) because of the large refractive index mismatch at the boundaries.

Finally, we have calculated the size dependence of the Rabi splitting of the ground-state polariton for the structures studied in the present experiments. The field distributions were obtained by fitting the results of our numerical calculations. In the unpatterned lower mirror we represent the fields for $|x,y|>L/2$ as products of exponentials and trigonometric functions that are determined from the boundary conditions. The resulting Ω for the (0,0,0) polariton is shown by the solid line in Fig. 8(b) together with the experimental results. The values for the Rabi splitting of the higher polaritons were estimated by scaling the Ω for the (0,0,0) polariton by the dependence $\Omega \propto \sqrt{1/E(L)}$ given above in model 1. The resulting model curves for the size and mode dependence are shown by solid lines in Fig. 8(a).

Both the decrease of the Rabi splitting with size L and its decrease in going from the ground photon state to higher-lying states at a given L are accounted for reasonably well by this last model. Physically, the reason for the stronger dependence of the Rabi splitting on cavity size is that the fields in the present structures extend laterally in the lower mirror region beyond the etched region. For decreasing size these fields tend to be forced increasingly into this lower mirror region. This gives a decreasing exciton-photon overlap in the oscillator strength for decreasing size and leads to a smaller Rabi splitting. From the comparison of these calculations for the three different models here, we see that the exciton-photon interaction and the Rabi splitting can be modified by changes in the geometry of the cavities. In particular, we predict that they will increase for a given size L if the lower mirror is etched more deeply.

V. CONCLUSION

In summary, we have investigated the weak and strong interaction between zero-dimensional optical modes and exciton states in PD's. The size and shape dependence of the optical mode spectrum has been studied by PL experiments and modeled by numerical calculations. By varying the temperature the formation of cavity polaritons from different confined optical modes and the ground-state magnetoexciton is observed. The Rabi splitting between the polariton branches decreases systematically with decreasing dot size. For a given size Ω decreases with increasing photon eigenvalues. By comparison with model calculations, both effects are traced to size dependences of the exciton-photon coupling due to variations of the electric-field distributions.

ACKNOWLEDGMENTS

This work was supported by the Deutsche Forschungsgemeinschaft, the State of Bavaria, and the U.S. Office of Naval Research.

[1] C. Weisbuch, M. Nishioka, A. Ishikawa, and Y. Arakawa, Phys. Rev. Lett. **69**, 3314 (1992), and references therein.

[2] R. Houdré, C. Weisbuch, R. P. Stanley, U. Oesterle, P. Pellandini, and M. Ilegems, Phys. Rev. Lett. **73**, 2043 (1994).

[3] P. Goy, J. M. Raimond, M. Gross, and S. Haroche, Phys. Rev. Lett. **50**, 1903 (1983).

[4] R. G. Hulet, E. S. Hilfer, and D. Kleppner, Phys. Rev. Lett. **55**, 2137 (1985).

[5] G. Björk, S. Machida, Y. Yamamoto, and K. Igeta, Phys. Rev. A **44**, 669 (1991).

[6] T. Yamauchi and Y. Arakawa, Appl. Phys. Lett. **58**, 2339 (1991).

[7] F. De Martini and G. R. Jacobovitz, Phys. Rev. Lett. **60**, 1711 (1988).

[8] U. Mohideen, R. E. Slusher, F. Jahnke, and S. W. Koch, Phys. Rev. Lett. **73**, 1785 (1994).

[9] M. G. Raizen, R. J. Thompson, R. J. Brecha, H. J. Kimble, and H. J. Carmichael, Phys. Rev. Lett. **63**, 240 (1989).

[10] Y. Zhu, D. J. Gauthier, S. E. Morin, Q. Wu, H. J. Carmichael, and T. W. Mossberg, Phys. Rev. Lett. **64**, 2499 (1990).

[11] J. M. Gérard, D. Barrier, J. Y. Marzin, R. Kuszelewicz, L. Manin, E. Costard, Y. Thierry-Mieg, and T. Rivera, Appl. Phys. Lett. **69**, 449 (1996).

[12] J. P. Reithmaier, M. Röhner, H. Zull, F. Schäfer, A. Forchel, P. A. Knipp, and T. L. Reinecke, Phys. Rev. Lett. **78**, 378 (1997).

[13] M. Röhner, J. P. Reithmaier, A. Forchel, F. Schäfer, and H. Zull, Appl. Phys. Lett. **71**, 488 (1997).

[14] Strictly speaking, the laterally confined photons are strong resonances on the continuum of photon states due to coupling to photons in the vacuum surrounding the PD's.

[15] P. A. Knipp and T. L. Reinecke, Phys. Rev. B **54**, 1880 (1996).

[16] P. A. Knipp and T. L. Reinecke, in *Proceedings of the 23rd International Conference on the Physics of Semiconductors, Berlin, 1996*, edited by M. Scheffler and R. Zimmermann (World Scientific, Singapore, 1996), p. 3131.

[17] In circular structures the problem can be separated and solved analytically to give results that are equivalent to the numerical calculations. These solutions are $J_{n_\varphi}(r)\exp(\pm i n_\varphi \varphi)$ inside of the dot $r<R$ and $K_{n_\varphi}(r)\exp(\pm i n_\varphi \varphi)$ outside $r>R$, which have to be matched at the lateral sidewalls of the photonic dot according to the boundary conditions for the fields. In the case of perfectly reflecting sidewalls the boundary conditions simplify to $J_{n_\varphi}(r=R)=0$.

[18] *Handbook of Mathematical Functions*, Natl. Bur. Stand. Appl. Math. Ser. No. 55, edited by M. Abramowitz and I. E. Stegun (U.S. GPO, Washington, DC, 1982).

[19] R. Houdré, R. P. Stanley, U. Oesterle, M. Ilegems, and C. Weisbuch, Phys. Rev. B **49**, 16 761 (1994).

[20] T. A. Fisher, A. M. Afshar, D. M. Whittaker, M. S. Skolnick, J. S. Roberts, G. Hill, and M. A. Pate, Phys. Rev. B **51**, 2600 (1995).

[21] J. Tignon, P. Voisin, C. Delalande, M. Voos, R. Houdré, U. Oesterle, and R. P. Stanley, Phys. Rev. Lett. **74**, 3967 (1995); T. Tanaka, Z. Zhang, M. Nishioka, and Y. Arakawa, Appl. Phys. Lett. **69**, 887 (1996).

[22] In Ref. 12 a cavity containing three $In_xGa_{1-x}As$ QW's with slightly different In contents was used for fabrication of PD's. The exciton emission was significantly broader than in the present structure with a single quantum well. Therefore, strong-coupling effects were not observed in the structures in Ref. 12.

[23] A strong interaction can only occur between exciton and photon states of the same symmetry. This means that the center-of-mass wave function of the exciton has the same shape as the exciton wave function.

[24] S. Rudin and T. L. Reinecke (unpublished).